HOKKAIDO UNIVERSITY

Title	Mechanistic insights into heme-mediated transcriptional regulation via a bacterial manganese-binding iron regulator, iron response regulator (Irr)
Author(s)	Nam, Dayeon; Matsumoto, Yuki; Uchida, Takeshi et al.
Citation	Journal of Biological Chemistry (JBC), 295(32), 11316-11325 https://doi.org/10.1074/jbc.RA119.011855
Issue Date	2020-08-07
Doc URL	https://hdl.handle.net/2115/82428
Rights	This research was originally published in the Journal of Biological Chemistry. Dayeon Nam, Yuki Matsumoto, Takeshi Uchida, Mark R. O'Brian and Koichiro Ishimori. Mechanistic insights into heme-mediated transcriptional regulation via a bacterial manganese-binding iron regulator, iron response regulator (Irr) . J. Biol. Chem. 2020; Vol295:pp11316-11325 © the American Society for Biochemistry and Molecular Biology or © Dayeon Nam, Yuki Matsumoto, Takeshi Uchida, Mark R. O'Brian and Koichiro Ishimori.
Type	journal article
File Information	J. Biol. Chem. 295-32_11316-11325.pdf

Hokkaido University Collection of Scholarly and Academic Papers : HUSCAP

Mechanistic insights into heme-mediated transcriptional regulation via a bacterial manganese-binding iron regulator, iron response regulator (Irr)

Received for publication, November 13, 2019, and in revised form, June 15, 2020 Published, Papers in Press, June 17, 2020, DOI 10.1074/jbc.RA119.011855

Dayeon Nam[1], **Yuki Matsumoto**[1], **Takeshi Uchida**[1,2], **Mark R. O'Brian**[3], **and Koichiro Ishimori**[1,2,*]

From the [1]*Graduate School of Chemical Sciences and Engineering, Hokkaido University, Sapporo, Japan,* [2]*Department of Chemistry, Faculty of Science, Hokkaido University, Sapporo, Japan, and* [3]*Department of Biochemistry, Jacobs School of Medicine and Biomedical Sciences, University at Buffalo, Buffalo, New York, USA*

Edited by Ruma Banerjee

The transcription factor iron response regulator (Irr) is a key regulator of iron homeostasis in the nitrogen-fixating bacterium *Bradyrhizobium japonicum*. Irr acts by binding to target genes, including the iron control element (ICE), and is degraded in response to heme binding. Here, we examined this binding activity using fluorescence anisotropy with a 6-carboxyfluorescein-labeled ICE-like oligomer (FAM-ICE). In the presence of Mn^{2+}, Irr addition increased the fluorescence anisotropy, corresponding to formation of the Irr–ICE complex. The addition of EDTA to the Irr–ICE complex reduced fluorescence anisotropy, but fluorescence was recovered after Mn^{2+} addition, indicating that Mn^{2+} binding is a prerequisite for complex formation. Binding activity toward ICE was lost upon introduction of substitutions in a His-cluster region of Irr, revealing that Mn^{2+} binds to this region. We observed that the His-cluster region is also the heme binding site; results from fluorescence anisotropy and electrophoretic mobility shift analyses disclosed that the addition of a half-equivalent of heme dissociates Irr from ICE, likely because of Mn^{2+} release due to heme binding. We hypothesized that heme binding to another heme binding site, Cys-29, would also inhibit the formation of the Irr–ICE complex because it is proximal to the ICE binding site, which was supported by the loss of ICE binding activity in a Cys-29–mutated Irr. These results indicate that Irr requires Mn^{2+} binding to form the Irr–ICE complex and that the addition of heme dissociates Irr from ICE by replacing Mn^{2+} with heme or by heme binding to Cys-29.

Iron is a necessary micronutrient for all organisms, as it plays a key role in cellular functions, acting as a chemical catalyst in addition to influencing electron transport, oxygen transport, and mitochondrial energy generation (1). However, excessive intracellular iron is cytotoxic; this is because of its ability to convert molecular oxygen into reactive oxygen species (ROS) that can cause damage to cellular components. Because of this, iron homeostasis is strictly regulated, and iron acquisition, storage, and consumption are balanced to maintain a constant cellular iron level (2). Defects in this regulation lead to severe diseases, such as anemia, pica, liver cirrhosis, and neurological deficits. Despite its biological importance, the molecular control mechanisms of iron homeostasis are still undiscovered, and functional characterization of the essential regulatory proteins is also still quite limited.

To investigate the molecular mechanisms of cellular iron homeostasis, *Bradyrhizobium japonicum*, a nitrogen-fixing bacterium that exists as an endosymbiont in root nodule of plants, is used as the typical model system. In this species of bacteria, various types of iron-containing proteins or heme, which is an iron-protoporphyrin IX complex, are used to support nitrogen fixation. The nitrogenase complex, which comprises more than 10% of cellular proteins in nitrogen-fixing bacteria, such as some cyanobacteria and azotobacteraceae, includes 30–34 iron ions per molecule (3). *B. japonicum* is known to possess a global regulator protein, known as the iron response regulator (Irr), which regulates iron homeostasis and associated metabolic processes (4–6). When cells are grown under iron-limiting conditions, Irr functions as a transcriptional repressor of the *hemB* gene, which encodes one of the heme biosynthetic enzymes, δ-aminoleuvulinic acid dehydratase; this prevents accumulation of a cytotoxic heme precursor, protoporphyrin IX. Under iron-replete conditions, Irr is thought to degrade, allowing *hemB* transcription to resume and promoting heme biosynthesis (7–9).

Using a yeast one-hybrid system, the *in vivo* interaction of Irr with the iron control element (ICE), which is an incomplete inversed repeat *cis*-performing AT-rich DNA region, has been reported (10). This motif is located upstream of Irr- and other iron-regulated genes (4, 11), and two *B. japonicum* genes that contain ICE-like motifs within their promoter regions were previously shown to be negatively regulated by Irr (4, 11, 12). By occupying the promoter-binding site in iron-limited cells, Irr represses gene transcription (12). The mRNA transcripts of Irr-regulated genes as well as the promoter occupancy by Irr were only seen under iron-depleted conditions, indicating that the interactions between Irr and the ICE-like motif depend on the iron status of the cells.

Interestingly, interactions between Irr and the ICE-like motif are also dependent on manganese (Mn^{2+}) (12). In media supplemented with Mn^{2+}, genes including ICE-like motifs were strongly regulated by iron, whereas this iron-dependent regulation was lost under low-manganese conditions. Thus, Mn^{2+} contributes to the expression of genes including ICE-like motifs, suggesting that the binding of Irr to the ICE-like motifs

* For correspondence: Koichiro Ishimori, koichiro@sci.hokudai.ac.jp.

Downloaded from http://www.jbc.org/ at HOKKAIDO DAIGAKU on October 11, 2020

© 2020 Nam et al. Published under exclusive license by The American Society for Biochemistry and Molecular Biology, Inc.

requires Mn^{2+} binding to Irr. Despite this evidence, Mn^{2+} binding to purified Irr protein has not yet been confirmed.

To detect the iron status of the intracellular environment, Irr has been found to utilize heme as a regulatory molecule (8). Irr degrades in iron-replete cells, restarting transcription of the genes it was repressing; this degradation is thought to be induced by the direct binding of heme. Irr has two heme binding sites, the first of which is Cys29 in the heme-regulatory motif (HRM), which contains a short consensus sequence composed of Cys and Pro and is found in many heme-regulated proteins, such as heme-regulated inhibitor kinases (13), heme activator proteins (14), and circadian factors (15). The other heme binding site is in the His-cluster region far from the HRM region. Heme binding to these sites in Irr induces the oxidative modification of the protein moiety, leading to Irr degradation (9).

It should be noted here that heme binding to Irr and the successive oxidative modification are inhibited in the presence of Mn^{2+}, and that the addition of Mn^{2+} to heme-bound Irr releases the heme from the protein (16). In a heme-deficient mutant strain, Δ*hemAH*, the addition of Mn^{2+} suppressed the degradation of Irr under the moderated heme concentrations (200 nM); however, cells grown under conditions with large excesses of heme (5 mM) did not accumulate Irr in the presence of Mn^{2+}, suggesting that the effectiveness of Mn^{2+} on preventing Irr degradation depends on the heme concentration (16). Therefore, Mn^{2+} is likely a competitive inhibitor of heme binding to the Irr protein; however, the binding site of Mn^{2+} in Irr has not yet been determined.

In this paper, we confirmed that the binding of Mn^{2+} is essential for Irr to bind to the ICE-like motif, using purified proteins and a fluorophore-labeled ICE-like oligomer DNA. The Mn^{2+} binding site was found to be in the His-cluster region of Irr, which overlaps one of the heme binding sites in Irr. Heme binding to Irr likely induces the release of Mn^{2+} from the binding site in the His-cluster region, dissociating Irr from the ICE-like motif. In addition, the conformational changes associated with heme binding to another heme binding site, Cys29 in the HRM region located near the ICE binding site, also inhibit binding to ICE. Although heme bound to Irr would trigger oxidative modification of the protein, which has been thought to be essential for the dissociation of Irr from the ICE-like motif, the heme-induced oxidative modification would be initiated after the dissociation of Irr from the target gene to protect the target gene from the ROS produced by heme-bound Irr. Because of this, the oxidative modification and protein degradation would inhibit the rebinding of Irr to the target gene and/or the formation of cytotoxic free heme.

Results and discussion

Effects of Mn^{2+} on Irr-ICE binding

Previous studies have reported that the promoter occupancy for genes including ICE-like motifs was suppressed under Mn^{2+}-limited conditions, suggesting that Mn^{2+} binding is essential for the binding of ICE to Irr (16). To confirm this, a 6-carboxyfluorescein-modified DNA oligomer (FAM-ICE) was prepared as a model for the ICE-like motif, and the formation of the complex between Irr and FAM-ICE was monitored using fluorescence anisotropy. In the presence of Mn^{2+}, fluorescence anisotropy of FAM-ICE was increased by the addition of Irr, corresponding to complex formation (Fig. 1, *green*). In the absence of Mn^{2+}, this increase was much smaller than that in the presence of Mn^{2+} (Fig. 1, *orange*), indicating that binding of the ICE-like motif to Mn^{2+}-free Irr was nonspecific and Mn^{2+} is essential for Irr to bind to the ICE-like motif.

The Mn^{2+}-mediated binding of Irr to ICE was also confirmed by the addition of a metal chelator, EDTA, to the Irr-ICE complex. When EDTA was added to the Irr-ICE complex, fluorescence anisotropy of FAM-ICE was decreased (Fig. 2*A*), indicating that removal of Mn^{2+} led to dissociation of Irr from FAM-ICE. The inductively coupled plasma-optical emission spectrometer (ICP-OES) measurements confirmed the complete dissociation of Mn^{2+} from Irr after the EDTA treatment (Table 1). Supporting this, in the presence of FAM-ICE, the addition of Mn^{2+} to Mn^{2+}-free Irr enhanced the fluorescence anisotropy, indicating that Mn^{2+} restored the binding ability of Irr (Fig. 2*B*). This type of essential role for metal binding in the binding activity to target DNA for transcriptional regulators is one of the characteristics of metal-responsive transcriptional regulators, including Fur. The apo (metal-free) state of *Magnetospirillum gryphiswaldense* MSR-1 Fur (*Mg*Fur) is unable to bind to the target DNA site; however, metal binding results in the restoration of this activity (17, 18). The binding of two metal ions to apo *Mg*Fur stabilizes the hinge conformation associated with conversion of the DNA binding domain into its DNA binding state.

To determine the Mn^{2+}-binding affinity of Irr, competition experiments with a fluorimetric dye, Mag-fura-2 (19), were carried out. However, the competition experiments required excess amounts of Mn^{2+}-free Irr to that of the dye, and rather higher concentrations of Mn^{2+}-free Irr (>10 μM) resulted in less accurate estimation of $K_{d(Mn^{2+})}$, varying from the nM to μM range because of the structural instability of Irr under the high-concentration range. The Mn^{2+} binding affinity of Irr seemed rather high compared with those of other Fur family proteins, such as *Escherichia coli* Fur (*Ec*Fur) [$K_{d(Mn^{2+})}$, 24 μM] (20) and manganese transport regulator (MntR) [$K_{d(Mn^{2+})}$, 50 and 160 μM] (19), which would be close to the heme binding affinity of Irr [$K_{d(heme)}$, 1 and 80 nM for two heme binding sites] (21). The comparable Mn^{2+} affinity to the heme binding affinity of Irr was supported by the competitive binding between heme and Mn^{2+}. As previously reported (16), the addition of 20 μM Mn^{2+} to 4 μM heme-bound Irr completely displaced heme from Irr.

The metal binding in Fur superfamily proteins also affects oligomerization status to regulate the binding affinity to target DNA (22). We examined the oligomerization status of Irr upon the binding of Mn^{2+} using size-exclusion column chromatography. Fig. 3*A* shows chromatograms for Irr in the absence and presence of Mn^{2+}; a major peak appeared at 14.7 ml, corresponding to an estimated molecular mass of 40 kDa (Fig. 3*B*). As the calculated molecular mass of monomeric Irr is 18 kDa, this result indicates that the Mn^{2+}-bound and Mn^{2+}-free Irr forms dimers. Irr, therefore, forms a stable dimeric state, which is similar to that seen in the group including *Ec*Fur (23) and *Helicobacter pylori* Fur (*Hp*Fur) (24).

Downloaded from http://www.jbc.org/ at HOKKAIDO DAIGAKU on October 11, 2020

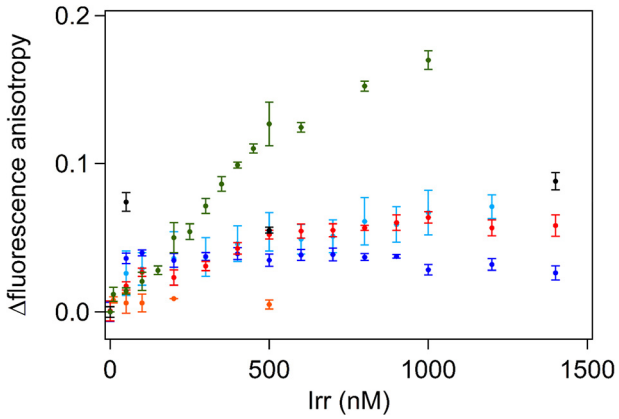


Figure 1. Irr titration to ICE. The fluorescence anisotropy changes for Irr WT with Mn^{2+} (*green*), C29A (*light blue*), H63A (*blue*), H117-119A (*black*), heme-bound Irr (*red*), and Mn^{2+}-free Irr (*orange*). The reaction solution contained 0–1,400 nM protein and 0.5 nM FAM-ICE. After 10 min of incubation at 25 °C, fluorescence anisotropy was measured by excitation at 495 nm and emission at 515 nm.

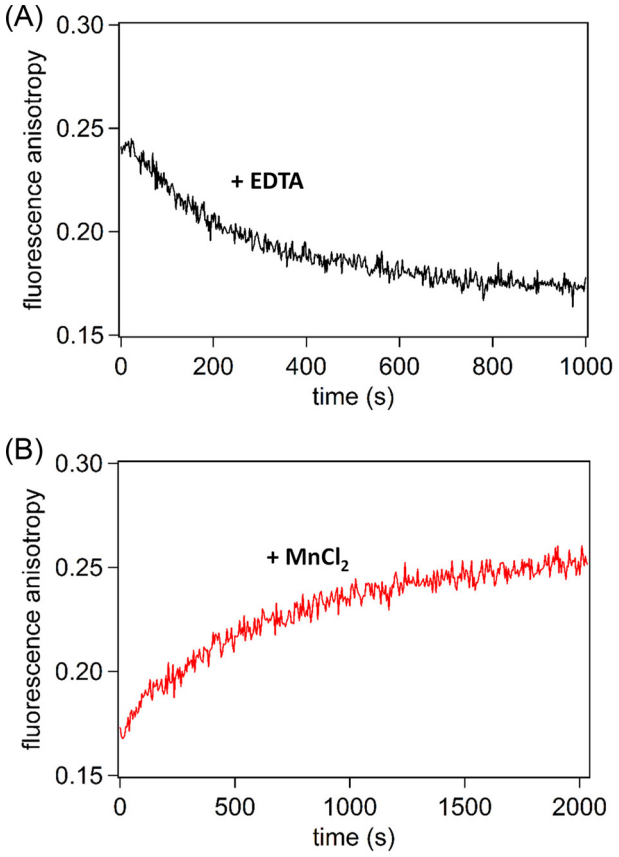


Figure 2. Time course of fluorescence anisotropy for FAM-ICE in the presence of Irr by addition of EDTA and $MnCl_2$. *A*, the change of fluorescence anisotropy for 0.5 nM FAM-ICE in the presence of 1 μM Irr and 10 μM Mn^{2+} by the addition of EDTA. The EDTA concentration was 1 mM. *B*, the change of fluorescence anisotropy for FAM-ICE in the presence of Irr by the addition of $MnCl_2$. 10 equivalents of $MnCl_2$ was added to Mn^{2+}-free Irr. The concentrations of Irr and FAM-ICE are 1 μM and 0.5 nM, respectively.

In the chromatogram of Mn^{2+}-free Irr, two additional peaks around 12.4 and 17.3 ml were observed, indicating the appearance of high- and low-molecular-mass species of Irr in the solution without Mn^{2+}. In the presence of EDTA, Mn^{2+}-free Irr was unstable and gradually formed precipitates under the concentrated conditions. The appearance of the high-molecular-mass species suggested the formation of oligomers by partially denatured Irr during gel chromatography. On the other hand, the reasons for the appearance of the low-molecular-mass species are unclear. Because the apparent molecular mass of the low-molecular-mass species was less than that of monomeric Irr, the interaction between partially denatured Irr and gels in column may retard the moving of the protein, resulting in the slow-moving species in the chromatogram. That the longer incubation with EDTA before applying the column enhanced the intensity of the low-molecular mass species also supports the gradual denaturation of Irr in the absence of Mn^{2+}. A trough around 18 ml also would be because of perturbations of the column conditions induced by nonspecific interactions between partially denatured Irr and gels in the column.

Table 1
Mn^{2+} binding property of Irr

Protein	Mn^{2+} content (mol/monomer)
Holo-Irr	1.82 ± 0.32
Apo-Irr	<0.1
Heme–Irr complex	<0.1
C29A	2.08 ± 0.23
H63A	<0.1
H117-119A	0.44 ± 0.07

Mn^{2+} binding site in Irr

The Fur superfamily has two metal binding sites (25). Site 1 is found in the C-terminal dimerization domain, and site 2 is found in the histidine-rich hinge region, known as the His-cluster region, between the DNA binding and dimerization domains. To confirm the metal binding to purified Irr, we utilized ICP-OES, which showed that Irr incubated with 0.1 mM $MnCl_2$ contained 1.82 ± 0.32 mol Mn/mol protein (Table 1). Other metals were present at less than 0.1 mol metal/mol protein. Although we found that Irr as isolated bound Zn^{2+}, the binding affinity of Zn^{2+} to Irr was much lower than that of Mn^{2+}, and incubation of purified Irr in a solution containing 0.1 mM $MnCl_2$ completely replaced Zn^{2+} with Mn^{2+}. The functional significance of the binding of Zn^{2+} in Irr as isolated is unclear, and considering that the expression level of Irr and the ICE binding depended only on Mn^{2+}, not on Zn^{2+}, in *B. japonicum* (16), and overexpressed *Bacillus subtilis* Fur (*Bs*Fur) incorporated Zn^{2+} into the metal binding site (26), the Mn^{2+} binding sites of newly synthesized Irr in cells was occupied by Zn^{2+} because of the overexpression of Irr and the abundance of Zn^{2+} in *E. coli* cells (27).

*Mg*Fur, one of the Fur proteins possessing two metal binding sites, similarly has two metal binding sites; site 1 is in the dimerization domain (*green*), and site 2 is in the histidine-rich hinge region (*gray*) near the DNA binding domain (*blue*) (Fig. 4). The amino acid residues His33, Glu81, His90, and Glu101, which constitute the histidine-rich hinge region in *Mg*Fur, are conserved in Irr (17), corresponding to His63, Asp111, His119, and Asp130, respectively. Most of the amino acid residues forming these two metal binding sites are conserved across all Fur superfamily proteins. For *Bacillus subtilis* PerR (*Bs*PerR), which is one of the Fur superfamily proteins and an iron-dependent peroxide sensor, functional characterization using mutant

Downloaded from http://www.jbc.org/ at HOKKAIDO DAIGAKU on October 11, 2020

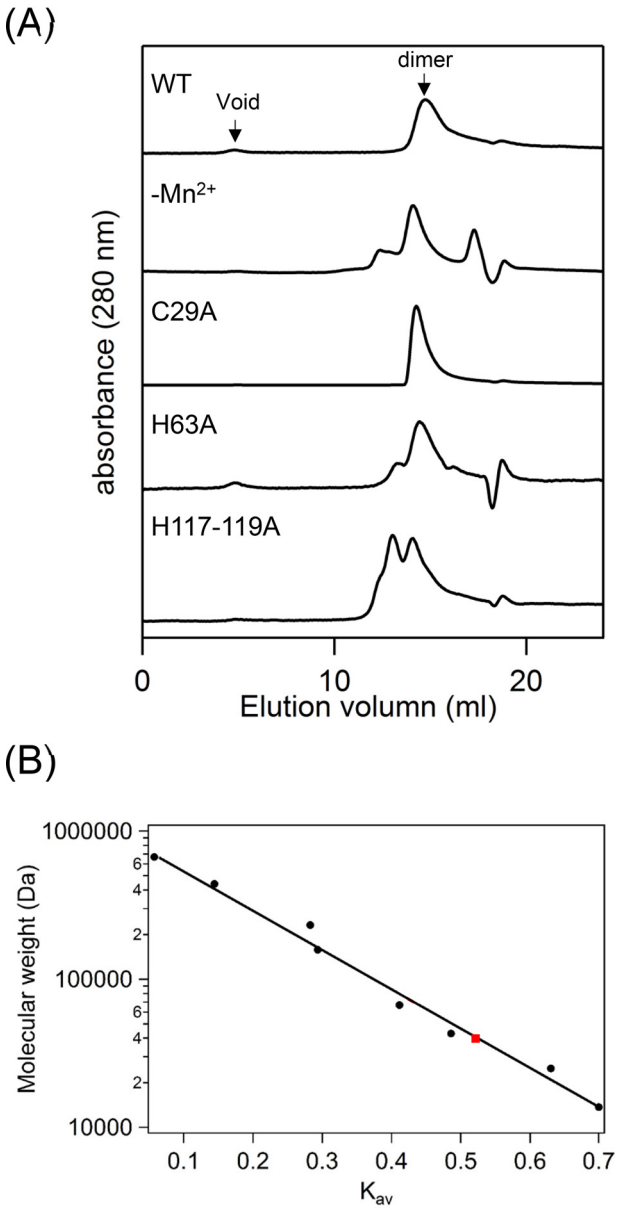


Figure 3. Size-exclusion chromatogram for Irr in the presence and absence of manganese and Irr mutants. *A*, the Irr solution in the presence (WT) or absence ($-Mn^{2+}$) of Mn^{2+} and Irr mutant solutions of C29A, H63A, and H117-119A were applied to the size-exclusion column (Bio-Rad, SEC650) equilibrated with 10 mM Tris-HCl, 100 mM NaCl, 10% glycerol at pH 8.0 with and without 100 μM $MnCl_2$. 120 μl of sample solution containing 10–50 μM protein was used for the measurements. Irr was detected by the absorbance at 280 nm. *B*, the linear calibration curve determined by the standard proteins. The peak at 14.7 ml corresponds to the molecular weight of 40 kDa (*red square*), showing that Irr forms dimers.

proteins (24, 28), crystal structures (29), and *in silico* study of free energy calculations, including molecular dynamics (30), revealed that metal occupancy at site 2 is necessary for the conformational changes required for binding to the operator sequence of genes. Although the metal binding sites in Irr have not yet been identified, the consensus amino acid sequence for site 2 in *Bs*PerR is completely conserved in this protein, suggesting that Mn^{2+} binds to site 2 in a similar manner in Irr.

To confirm Mn^{2+} binding to site 2 in Irr, we mutated amino acid residues constituting this site (H63A and H117-119A). These His-cluster mutants were quite unstable at higher concentrations (>10 μM), and, as illustrated in Fig. 3*A*, high- and low-molecular-weight species were detected in the gel chromatogram, as found for Mn^{2+}-free Irr. Longer incubation of these mutants under high concentrations before applying the column resulted in aggregation and precipitation. In the His117-119A mutant, we detected substantial amounts of high-molecular-weight species, probably because of the aggregation of the partially denatured proteins. The destabilized structures of these mutants also suggest that the His-cluster region is the keystone for the protein structure of Irr.

On the other hand, no aggregation or precipitation was observed for these His-cluster mutants at lower concentrations (~1 μM), and the fluorescence anisotropy of FAM-ICE was measured during titration of these mutants to FAM-ICE using 1 μM Irr. As shown in Fig. 1 (*blue* and *black circles*), the increase of the fluorescence anisotropy by the addition of Irr in the presence of Mn^{2+} was significantly suppressed for both mutants compared with the WT protein, indicating the mutant proteins failed to convert into the conformer suitable for DNA binding; this suggests that Irr binds Mn^{2+} at site 2 in the His-cluster region of Irr, and that this binding is essential for ICE binding. The ICP-OES measurements for these His-cluster mutants revealed reduced amounts of the Mn^{2+} contents (Table 1), which also supports the Mn^{2+} binding at site 2 in the His-cluster region.

Effects of heme binding on Irr-ICE complex formation

As previously reported, Irr utilizes heme as the regulatory molecule for the cellular iron status, and, under iron-replete conditions, Irr binds heme to inhibit binding to the ICE-like motif and to dissociate from the ICE-like motif (9). Because one of the heme binding sites is located in the His-cluster region in Irr (6), one possible mechanism of heme-induced inhibition of binding to the ICE-like motif and dissociation of Irr from the ICE-like motif is that heme binding to the His-cluster region in Irr induces the release of Mn^{2+} from site 2, which then triggers the inhibition of binding to the ICE-like motif and dissociation of Irr from the ICE-like motif.

The heme-induced inhibition of binding to the ICE-like motif in Irr was confirmed by using electrophoretic mobility shift analysis (EMSA). As illustrated in Fig. 5*A*, the band with slower mobility was enhanced with increased concentrations of Irr (0, 1, 2.5, 5, 10, 15, 20, 30, 40, and 50 nM) with the compensation of the intensity of the fast-moving band from the unbound ICE-like motif. This band shift corresponds to complex formation between Irr and the ICE-like motif. On the basis of the band intensities, the dissociation constant for ICE binding to Irr [$K_{d(\mathrm{Irr,ICE})}$] was estimated to be 15.7 ± 0.7 nM (Fig. 5*B*), consistent with the previous report (12). Although the fluorescence anisotropy measurements (Fig. 1) also provide the $K_{d(\mathrm{Irr,ICE})}$ value, the accurate determination failed because of the nonspecific changes of the fluorescence anisotropy, as observed for the Mn^{2+}-free and mutant Irr.

In the presence of heme, only a single band with faster mobility appeared (Fig. 5*C*). The intensities of the faster mobility bands in the presence of heme were comparable with those in

Downloaded from http://www.jbc.org/ at HOKKAIDO DAIGAKU on October 11, 2020

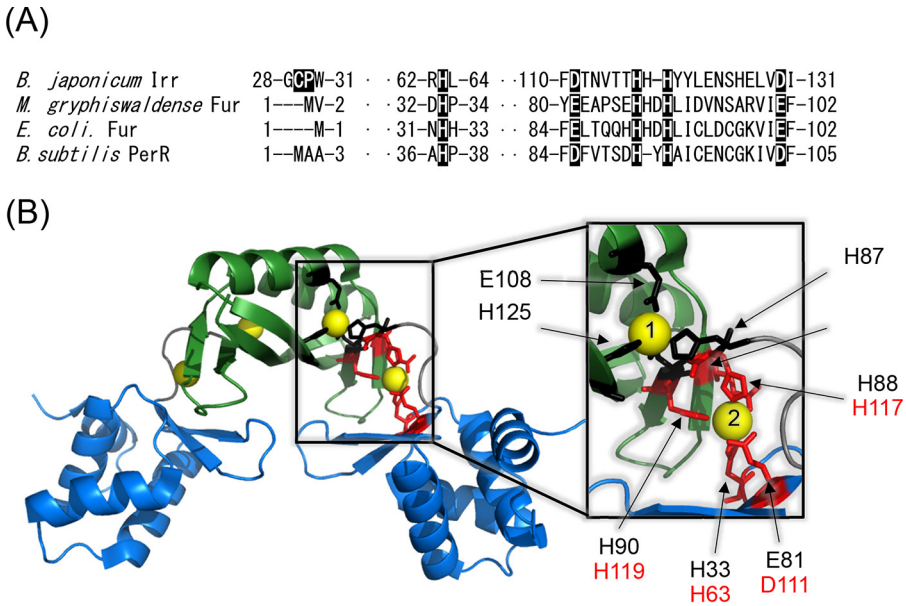


Figure 4. The sequence alignment of Fur family and the X-ray structure of *Mg*Fur (Protein Data Bank code 4RAZ). *A*, the *black* background is the predicted metal binding sites and sequence identity. *B*, *Mg*Fur is composed of a dimerization domain (*green*), hinge (gray), DNA binding domain (*blue*), and Mn^{2+} (*yellow*). In the protein structure, ligands for site 2 for Mn^{2+} are near the hinge. The *black* and *red* residue numbers of metal ligand correspond to *Mg*Fur and Irr, respectively.

the absence of heme (Fig. 5*A*), indicating that the binding to the ICE-like motif was completely inhibited by the addition of heme. Thus, we can conclude that heme binding to Irr inhibits the binding of the ICE-like motif to Irr.

To examine the heme-induced dissociation of Irr from the ICE-like motif, we measured fluorescence anisotropy changes associated with the titration of heme to the Irr-ICE complex. As depicted in Fig. 6, the addition of heme to the Irr-ICE complex decreased the fluorescence anisotropy, clearly showing the heme-induced dissociation of Irr from the ICE-like motif. Note that the decrease of the fluorescence anisotropy was almost constant after the addition of a half-equivalent of heme, implying that this was enough for the full dissociation of Irr. Considering that Irr forms dimers, as shown in Fig. 3, and a half-equivalent of heme dissociates the ICE-like motif from Irr, the dissociation constant [$K_{d(\text{Irr-ICE,heme})}$] for the heme binding to the Irr-ICE complex, which can be defined in the following reaction, was estimated.

$$\text{Heme} + (Mn^{2+}\text{-Irr-ICE})_2 \overset{K_{d(\text{Irr-ICE, heme})}}{\rightleftharpoons} [\text{Heme-}(Mn^{2+}\text{-Irr-ICE})_2]$$

$$\xrightarrow{\text{fast}} \text{Heme-Irr}_2 + 2\ Mn^{2+} + 2\ \text{ICE}$$

In this reaction Scheme, the heme-bound Irr-ICE complex would immediately release Mn^{2+} from the complex, resulting in the dissociation of the fluorophore-labeled ICE-like motif from heme-bound Irr. The concentration of the transient heme-bound Irr-ICE complex can be estimated from the fluorophore-labeled ICE-like motif. Thus, the equation for the single binding model, Equation 2 in Materials and methods, can be used to estimate $K_{d(\text{Irr-ICE, heme})}$. The calculated $K_{d(\text{Irr-ICE, heme})}$ value was 74 ± 13 nM, which is comparable with the dissociation constant of one of the heme binding sites [$K_{d(\text{heme})}$] in the absence of the ICE-like motif (80 nM) (8), suggesting that the Mn^{2+} binding sites are located near one of the heme binding sites and supporting the Mn^{2+} binding site in the His-cluster region, one of the heme binding sites of Irr.

The heme-induced dissociation of Mn^{2+} from the binding sites of Irr is also confirmed by the ICP-OES measurements. In the presence of heme, the ICP-OES measurements revealed that only less than 0.1 mol Mn/mol protein was bound to Irr (Table 1). The heme binding to Irr, therefore, seriously affected the metal binding sites, which almost completely dissociated Mn^{2+} from Irr. Such metal displacement was also reported for site 2 of *Hp*Fur (24). *Hp*Fur has three Zn^{2+} binding sites, but site 2 is the only site that can be replaced by another metal ion. Considering that metalation of site 2 triggers a conformational change to a conformation suitable for specific interaction with target DNA, it is more plausible that the heme binding, concomitant with release of Mn^{2+} from site 2, converts the protein structure into one not suitable for target DNA binding.

It should be noted here that another heme binding site in Irr is Cys29, which is located close to the ICE binding site (6); this suggests that the heme binding to Cys29 would perturb the conformation of the ICE binding site, resulting in the dissociation of Irr from the ICE-like motif. The conformational effects of Cys29 on the ICE binding was evident by the suppression of the ICE binding in the Cys29 mutant. We prepared a mutant having an Ala residue at position 29 (C29A) and monitored the fluorescence anisotropy change of FAM-ICE when the Cys29 mutant was added. Unlike WT Irr (Fig. 1, *green*), the addition of the Cys29 mutant (Fig. 1, *light blue*) showed only a small increase in anisotropy, indicating the suppression of ICE binding and suggesting that the mutation at Cys29 displaced Mn^{2+} in the His-cluster region of Irr to inhibit the ICE binding to Irr. However, the Mn^{2+} contents were unchanged by the mutation

Downloaded from http://www.jbc.org/ at HOKKAIDO DAIGAKU on October 11, 2020

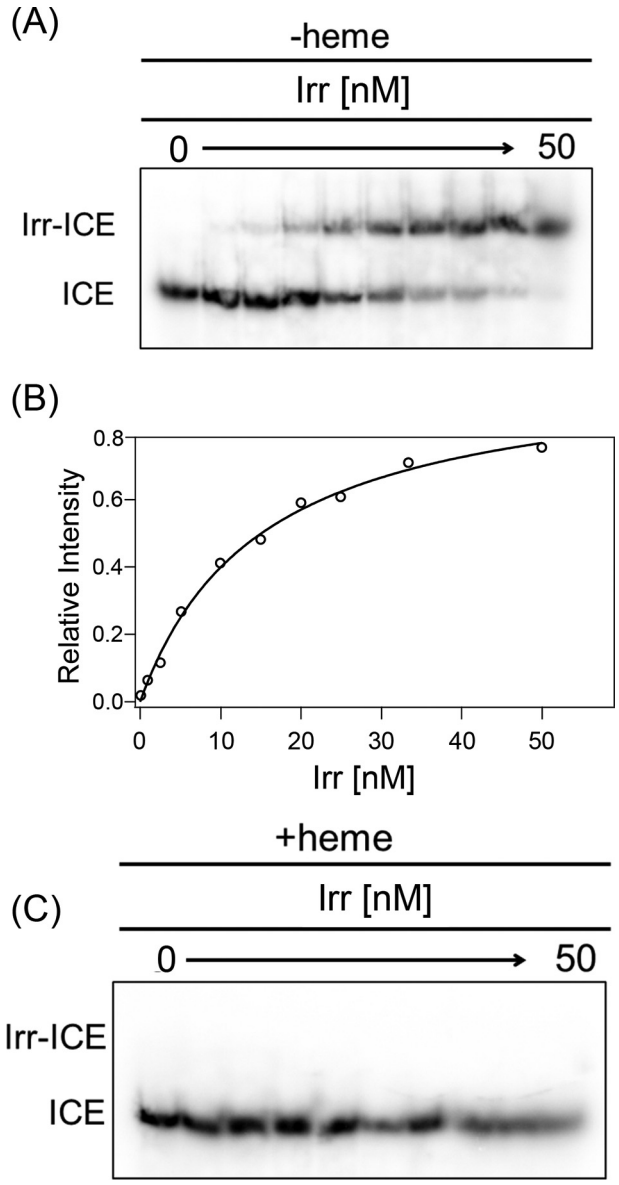


Figure 5. EMSA for Irr-ICE complex formation. *A*, gel image of ^{32}P-labeled ICE in the presence of 0, 1, 2.5, 5, 10, 15, 20, 30, 40, and 50 nM Irr. *B*, relative intensities of the bands from the Irr-ICE complex (*open circle*) and the fitting curve as described in Materials and methods. The band intensities estimated by ImageJ software and the relative intensity of the band in the absence of Irr were set to 1. The dissociation constant for the binding of ICE-like motif to Irr [$K_{d(Irr,ICE)}$] was estimated using a linear least-square method. *C*, gel image of ^{32}P-labeled ICE in the presence of 100 μM heme and the same concentrations as those described above.

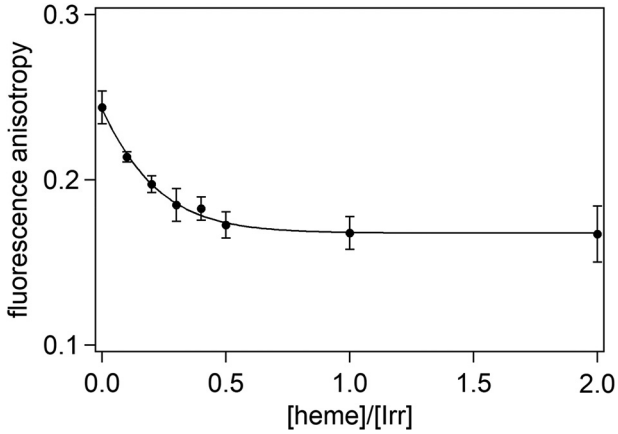


Figure 6. Fluorescence anisotropy changes by addition of heme to Irr-ICE complex. The reaction solution contained 1 μM Irr and 0.5 nM FAM-labeled ICE. The fluorescence anisotropy at 515 nm was measured by excitation at 495 nm after 10 min of incubation with heme at 25 °C.

at Cys29 (Table 1), suggesting that, by being in close proximity to the ICE-like motif, conformational changes induced by the mutation at Cys29 inhibited the binding to the ICE-like motif without the dissociation of Mn^{2+} from the His-cluster.

Another function of heme bound to Irr is the generation of ROS. As previously reported (31), heme binding to Irr resulted in the oxidative modification of the protein moiety in the presence of a reducing agent, leading to the loss of target DNA binding activity. However, the reaction mixture for the fluorescence anisotropy in Fig. 6 did not contain any reducing agents, such as dithiothreitol (DTT), which are required for the generation of ROS and oxidation of amino acid residues. The heme-induced oxidative modification was also found in iron regulatory protein 2 (IRP2) (32), which is recognized by E3 ubiquitin ligase for protein degradation in a ubiquitin-proteasome system (33); these oxidative modifications of the protein moiety and the successive protein degradation have been believed to be essential for regulation mechanisms. However, we recently reported that the release of IRP2 from the target RNA requires only direct heme binding to IRP2 but not heme-induced oxidative modification and protein degradation (34).

The functional advantage of the dissociation mechanism without oxidative modification would be the protection of the target gene or mRNA from ROS. In the oxidative modification of Irr, we identified the production of H_2O_2 and further activation of H_2O_2 to more reactive species, such as hydroxyl radicals, which oxidized amino acid residues near the His-cluster region (31). However, ROS produced in the ICE-bound Irr would also damage the target gene, as already reported (35). To protect the target gene, it is more reasonable that the oxidative modification would be induced after the release of the target gene from Irr.

Conformational effects of heme binding on Irr

To gain insights into the heme-induced structural changes in Irr that inhibit target DNA binding, we measured the CD spectral changes induced by the addition of heme. As displayed in Fig. 7*A*, the addition of heme resulted in the decrease of the negative ellipticity in the region from 205 to 230 nm, showing significant perturbations in the secondary structure of Irr. The decreased negative ellipticity at 222 nm corresponds to the reduction of α-helical contents from 14 to 6% that occurred with increasing heme from 0 to 10 equivalents. Considering that metal binding site 2 is located in the hinge region regulating the conformation of the DNA binding domain, the significant decrease of the α-helical contents associated with heme binding corresponds to conformational perturbations of the DNA binding domain (25). Such decreased negative ellipticity was also observed for the Mn^{2+} binding to Irr (16), and loss of Mn^{2+} in the His-cluster region resulted in the enhanced ellipticity in the region from 210 to 230 nm, as found for the C29A

Downloaded from http://www.jbc.org/ at HOKKAIDO DAIGAKU on October 11, 2020

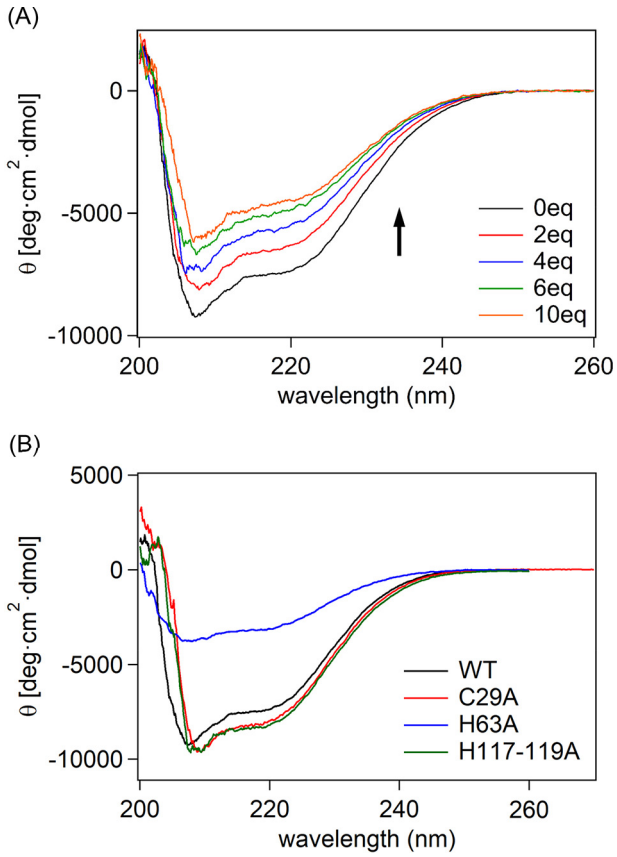


Figure 7. CD spectra of Irr mutants and CD spectral changes in Irr by addition of heme. *A*, CD spectra of Irr were recorded in the absence (*black*) and presence (*red*, *blue*, *green*, and *orange*, representing 2, 4, 6, and 10 equivalents, respectively) of heme. The sample concentration is about 5 μM Irr in 50 mM NaPi, pH 8.0, at room temperature. *B*, CD spectra of Irr (*black*) and the C29A, H63A, and H117-119A mutants (*red*, *blue*, and *green*, respectively) are shown. The sample concentration is about 5 μM Irr mutant in 50 mM NaPi, pH 8.0, at room temperature.

and H117-119A mutant (Fig. 7*B*). On the other hand, another His-cluster mutant, H63A, showed drastically decreased negative ellipticity (Fig. 7*B*), probably because of the low structural stability of the mutant. Such a destabilized protein structure having a tendency to be partially denatured was also suggested by the appearance of the high- and low-molecular-weight species in its gel filtration (Fig. 3*A*). The similar CD spectral changes with heme and Mn^{2+} binding suggest that the heme binding site overlaps the Mn^{2+} binding site, supporting the replacement of Mn^{2+} with heme.

Whereas both heme and Mn^{2+} binding reduced the α-helical contents in Irr, the Mn^{2+} binding to *Ec*Fur resulted in the increase of the α-helical contents, whereas the α-helical content was decreased by the binding of heme (16). One of the reasons for the opposite effect of Mn^{2+} binding on the CD spectra between *Ec*Fur and Irr would be the differences in the Mn^{2+} binding site. In *Ec*Fur, the reversible metal binding site is reported to be constituted by His31, His32, and His131 (36), which is different from the composition of Irr site 2. These differences would result in different conformational changes, corresponding to the opposite spectral changes in the CD spectra.

Although heme and Mn^{2+} binding induced similar CD spectral changes in Irr, the effects of heme binding to the ICE-like

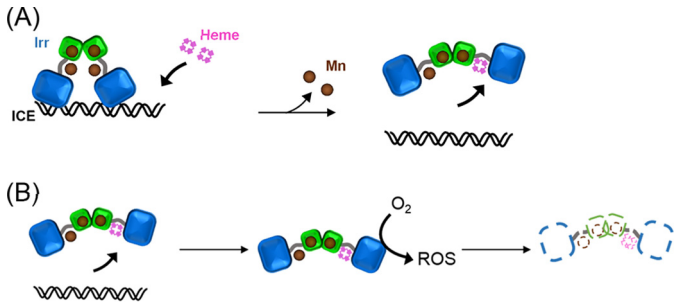


Figure 8. A proposed mechanism of heme-induced dissociation of Irr from the ICE-like motif in the target gene and heme-induced oxidative modification. *A*, Irr is composed of a dimerization domain (*green square*), hinge (*gray curve*), DNA binding domain (*blue square*), and Mn^{2+} (*brown circle*) based on *Mg*Fur. Irr dissociates from the ICE-like motif in the target gene (*black curve*) by the replacement of Mn^{2+} with heme (*pink*) in the His-cluster region (*gray curve*). Heme binding to Irr changes the conformation, and Irr becomes unstable to dissociate from the ICE-like motif. *B*, after the dissociation of Irr from the target gene, oxidative modification is induced, leading to protein degradation.

motif binding were completely different from those caused by Mn^{2+} binding; heme binding abolishes the ICE-like motif binding in Irr, whereas the ICE-like motif binding requires Mn^{2+} to bind. Because of the lack of the overall structure of heme- and Mn^{2+}-bound Irr, detailed structural perturbations induced by heme and Mn^{2+} binding to Irr are still unclear. However, one of the apparent structural differences between heme and Mn^{2+} binding is the size of these molecules, as heme is much larger than Mn^{2+}. Another major difference is the coordination number; five amino acid residues coordinate to the metal ion in Fur superfamily proteins, whereas heme is coordinated by only one or two amino acid residues (6). Therefore, the differences in the molecular size and coordination structure between heme and Mn^{2+} would reflect different perturbations in the conformations of the DNA binding domain of Irr, although both heme and Mn^{2+} binding decrease the α-helical contents.

Heme-induced dissociation mechanism of Irr from ICE-like motif

Based on the present data, we can propose a mechanism for the heme-induced dissociation of Irr from the ICE-like motif, as illustrated in Fig. 8. Irr consists of the dimerization domain (*green square*), hinge (*gray curve*), DNA binding domains (*blue square*), and Mn^{2+} (*brown circle*), as found for *Mg*Fur. At first, binding of heme to Irr releases Mn^{2+} from site 2 in the His-cluster region of the hinge, and the larger molecular size and different coordination structure of heme (pink color) compared with that of Mn^{2+} induces substantial structural changes in the His-cluster region. This facilitates the dissociation of Irr from the ICE-like motif without oxidative modification (Fig. 8*A*). As clearly shown in Fig. 6, a half-equivalent of heme was required for dissociation, indicating that the conformational changes by heme binding of one of the protomers in dimeric Irr would perturb the relative positions of two protomers, resulting in the destabilization of the dimeric forms for the binding of the target DNA and dissociation from the ICE-like motif. After heme-bound Irr dissociates from the ICE-like motif, heme in Irr is reduced, and molecular oxygen binds to the heme iron to be activated to form ROS (Fig. 8*B*). The generated ROS would

Downloaded from http://www.jbc.org/ at HOKKAIDO DAIGAKU on October 11, 2020

attack amino acid residues adjacent to the heme binding site in the His-cluster region (31), destabilizing the protein structure through oxidative modification and leading to protein degradation.

Although the functional significance of the oxidative modification and successive protein degradation as found for heme-bound Irr and IRP2 is still unclear, one of the possible reasons for inducing protein degradation would be to avoid the release of heme from the protein, as free heme is highly cytotoxic. As we previously reported (31), oxidative modification often leads to heme degradation as well as protein degradation, which drastically reduces the cytotoxicity of heme. To ensure the heme-induced regulation and suppress the cytotoxic effects of free heme, the heme-induced oxidative protein degradation would be required after the dissociation of Irr from the ICE-like motif.

In conclusion, Irr requires Mn^{2+} binding to form its DNA-bound complex, and the addition of heme replaces Mn^{2+} at site 2 in the His-cluster region, resulting in dissociation of Irr from the ICE-like motif in the target gene. Oxidative modification was not a prerequisite for dissociation of Irr from the ICE-like motif. The heme-induced oxidative modification would be initiated after the dissociation of Irr from the target gene to protect the target gene from ROS produced by heme-bound Irr, and oxidative modification followed by the degradation of the protein would inhibit the rebinding of Irr to the target gene as well as the formation of cytotoxic free heme.

Materials and methods

Protein expression and purification

The *irr* gene was amplified by PCR and cloned into the pETM-11 vector. Expression and purification of WT and mutant Irr were carried out as described previously (37). To completely replace Zn^{2+} with Mn^{2+} in Irr as purified, 10 μl of 0.5 M EDTA solution was added to 5 ml of the Irr solution and, after a 3-h incubation with mild stirring, the Irr solution was applied to the gel filtration column (ÄKTAprime plus system, GE Healthcare), the eluate was concentrated by ultrafiltration, and 0.7 μl of 0.1 M $MnCl_2$ solution was added to 0.5 ml of the Irr solution. The metal contents were then determined by ICP-OES measurements (Table 1). The concentration of Irr was determined on the basis of absorbance at 280 nm using an extinction coefficient of 18.3 mM^{-1} cm^{-1} (38). Irr mutants were constructed using a PrimeSTAR mutagenesis basal kit (Takara Bio). For the H117-119A mutant, a His_6 tag was attached to the C terminus for purification.

The presence of transition metal ions was determined by ICP-OES under operating conditions suitable for routine multielement analysis. The instrument was calibrated using 0, 0.001, 0.002, 0.005, 0.01, 0.02, and 0.05 mg/liter certified 100-mg Mn^{2+} and Zn^{2+} standard calibration solutions (Wako Pure Chemical Industries, Osaka, Japan). Before the ICP-OES measurements, protein samples were passed through a PD Minitrap G-25 column (GE Healthcare Bio-Sciences AB, Uppsala, Sweden) equilibrated with 50 mM HEPES, pH 7.5, to remove the excess amount of metal ions. All the protein samples were incubated for at least 30 min in a solution containing 0.1 mM $MnCl_2$ to completely replace Zn^{2+} with Mn^{2+}, which was confirmed by the ICP-OES measurements (typically, 1.82 ± 0.32 mol Mn/monomer and less than 0.1 mol Zn/monomer) before the spectroscopic measurements and gel chromatography.

Size-exclusion column chromatography

Size-exclusion experiments were performed at 4 °C with an ÄKTAprime plus system (GE Healthcare). Irr sample solutions were loaded on a size-exclusion column (Bio-Rad, SEC650) equilibrated with a standard buffer of 10 mM Tris-HCl, 100 mM NaCl, 10% glycerol, and 100 μM $MnCl_2$ (pH 8.0) at a flow rate of 1 ml min^{-1}. A heme solution was prepared at a concentration of about 500 μM in 0.1 M NaOH. Irr was detected by absorbance at 280 nm. Blue dextran (2,000,000 Da), ferritin (440,000 Da), catalase (232,000 Da), aldolase (158,000 Da), BSA (67,000 Da), ovalbumin (43,000 Da), chymotryosinogen (25,000 Da), and RNase (13,700 Da) were used for the standard samples. Blue dextran was used to determine column exclusion limits. The retention volumes observed for the standard proteins were transformed with the partial coefficient, K_{av} (39).

Fluorescence anisotropy spectroscopy

The target DNA oligomer used for the fluorescence anisotropy measurements was the ICE-like motif of the blr7895 gene (CAGAATTTAGAATCATTCTAAACTGAC) (4). A fluorescent group, 6-carboxyfluorescein (6-FAM), was covalently bound to the 5′ end of this synthetic oligomer, which was purchased from Eurofins Genomics at HPLC grade. The 6-FAM-labeled ICE-like motif of blr7895, designated FAM-ICE, was dissolved in 10 mM Tris-HCl, 150 mM NaCl, and 1 mM EDTA (pH 8.0). All buffers were sterilized using a 0.2-μm filter. After dissolving in a black microtube, FAM-ICE was annealed by heating to 95 °C for 5 min and cooled to room temperature for ~12 h. The prepared FAM-ICE was divided into 100-μl aliquots and stored at −20°C until further use.

The fluorescence anisotropy was recorded with an FP-8500 fluorometer (JASCO). The measurements were taken at excitation and emission wavelengths of 495 and 515 nm, respectively. The concentration of FAM-ICE for the titration with Irr was 0.5 nM. To monitor complex formation between Irr and FAM-ICE, Irr was titrated into a reaction mixture containing FAM-ICE, 50 mM HEPES, 10 mM KCl, 5% glycerol, 100 μM $MnCl_2$, and 1 mM $MgCl_2$ at pH 7.5, and the anisotropy was measured after 10 min of incubation for the formation of the Irr-ICE complex.

To monitor the heme-induced dissociation of FAM-ICE from Irr, 0.1, 0.2, 0.5, 1, and 2 equivalents of heme were added to the Irr-ICE complex solution. The sample contains 1.0 μM Irr and 0.5 nM 6-FAM-labeled ICE. The fluorescence anisotropy at 515 nm was measured by excitation at 495 nm after 10 min of incubation with heme at 25 °C. The data presented were averaged from three independent measurements. Total fluorescence anisotropy was calculated using Equation 1,

Downloaded from http://www.jbc.org/ at HOKKAIDO DAIGAKU on October 11, 2020

$$\text{Anisotropy} = \frac{I_{VV} - GI_{VH}}{I_{VV} - 2GI_{VH}} \quad \text{(Eq. 1)}$$

where I is fluorescence intensity, the first character of the subscript is polarization direction of the excitation light, and the second character is the direction of the emission. V and H mean the vertical and horizontal, respectively, and G is an instrument correction factor determined by excitation of the Irr solution with horizontally polarized light. $K_{d(\text{Irr-ICE,heme})}$ for the heme binding to the Irr-ICE complex was determined by using the following equation and the nonlinear least-squares method (IGOR Pro, Wavemetrics, Lake Oswego, OR):

$$FA = FA_0 + \Delta FA \frac{P_t + L_t + K_{d(\text{Irr-ICE,heme})} - \sqrt{\left(P_t + L_t + K_{d(\text{Irr-ICE,heme})}\right)^2 - 4P_tL_t}}{2P_t} \quad \text{(Eq.2)}$$

where FA is the fluorescence anisotropy at a given hemin concentration, FA_0 is the fluorescence intensity in the absence of hemin, ΔFA is the fluorescence anisotropy difference between Irr-bound and free fluorophore-labeled ICE-like motifs, and P_t and L_t are the total Irr and hemin concentrations, respectively.

EMSA

EMSA was used to observe the inhibition of the formation of the Irr-ICE complex by heme. Irr was incubated with 1 μg liter^{-1} (dI-dC)$_n$ · (dI-dC)$_n$ DNA, 100 μg ml^{-1} BSA, 100 μM $MnCl_2$, and 0.1 nM ^{32}P-radiolabeled ICE probe in a 20-μl volume of EMSA binding buffer (10 mM Bis-Tris borate, 1 mM $MgCl_2$, 40 mM KCl, 5% glycerol, 0.1% NP-40, 1 mM DTT, pH 7.5) for 30 min at room temperature.

After incubation for 30 min, the reaction mixtures were applied to 5% nondenaturing polyacrylamide gels in an electrophoresis buffer (20 mM Bis-Tris borate and 100 μM $MnCl_2$, pH 7.5) and were prerun for 30 min at a 220-V constant voltage and 4 °C. After the electrophoresis, gels were dried and autoradiographed. To observe the effect of heme, 2.5 mg ml^{-1} hemin solved in 50% ethanol–50% H_2O solution containing 0.02 N NaOH was added to the electrophoresis buffer. The intensities of the bands were quantitated by using ImageJ. The dissociation constant for the binding of the ICE-like motif to Irr ($K_{d(\text{Irr, ICE})}$) was estimated using Equation 3 and the nonlinear least-squares method (IGOR Pro, Wavemetrics, Lake Oswego, OR):

$$[\text{ICE}]I_{\text{Irr-ICE}} = \frac{[\text{Irr}] + [\text{ICE}]I_{\text{ICE}} + K_{d(\text{Irr,ICE})} - \sqrt{\left([\text{Irr}] + [\text{ICE}]I_{\text{ICE}} + K_{d(\text{Irr,ICE})}\right)^2 - 4[\text{Irr}][\text{ICE}]I_{\text{ICE}}}}{2} \quad \text{(Eq.3)}$$

where [Irr] is the concentration of Irr, [ICE] is the initial concentration of the fluorophore-labeled ICE-like motif, and $I_{\text{Irr-ICE}}$ and I_{ICE} are the normalized band intensities of the Irr-bound and free ICE-like motifs, respectively, at a given Irr concentration.

CD

CD spectra in the far-UV region were measured with a J-1500 CD spectrometer (JASCO) over the spectral range 200–250 nm at room temperature. Spectra were acquired at 0.2-nm intervals with a scan rate of 20 nm min^{-1} using a quartz cuvette with a path length of 10 mm; values presented are averages from three scans. The sample concentration was ~5 μM in 50 mM sodium phosphate (pH 8.0). A buffer spectrum measured under the same conditions was subtracted to obtain the actual sample spectrum. Two equivalents of heme were mixed with Irr, and after ~15 min at room temperature, the spectra were measured.

Data availability

All data are contained within the manuscript.

Acknowledgments—We thank the Open Facility, Global Facility Center, Creative Research Institution, Hokkaido University, for allowing us to conduct the analysis of Irr using ICP-OES and providing insight and expertise that greatly assisted the research.

Author contributions—D. N. and K. I. data curation; D. N., Y. M., and K. I. formal analysis; D. N. and K. I. funding acquisition; D. N., Y. M., and K. I. investigation; D. N., Y. M., and K. I. visualization; D. N. and K. I. writing-original draft; D. N., Y. M., T. U., M. R. O., and K. I. writing-review and editing; Y. M., T. U., and K. I. methodology; T. U. and K. I. conceptualization; T. U. and K. I. supervision; T. U., M. R. O., and K. I. validation; K. I. project administration; M. R. O. resources.

Funding and additional information—Funding was provided by Ministry of Education, Culture, Sports, Science and Technology (MEXT) of Japan (19H05769) and a National Institutes of Health Grant (R01 GM122947). The content is solely the responsibility of the authors and does not necessarily represent the official views of the National Institutes of Health.

Conflict of interest—The authors declare that they have no conflicts of interest with the contents of this article.

Abbreviations—The abbreviations used are: Irr, iron response regulator; ICE, iron control element; FAM-ICE, 6-carboxyfluorescein-attached ICE-like oligomer; ROS, reactive oxygen species; HRM, heme-regulatory motif; ICP-OES, inductively coupled plasma-optical emission spectrometer.

References

1. Aisen, P., Enns, C., and Wessling-Resnick, M. (2001) Chemistry and biology of eukaryotic iron metabolism. *Int. J. Biochem. Cell Biol.* **33,** 940–959 CrossRef Medline
2. Wang, J., and Pantopoulos, K. (2011) Regulation of cellular iron metabolism. *Biochem. J.* **434,** 365–381 CrossRef Medline
3. Eady, R. R. (1996) Structure−function relationships of alternative nitrogenases. *Chem. Rev.* **96,** 3013–3030 CrossRef Medline
4. Rudolph, G., Semini, G., Hauser, F., Lindemann, A., Friberg, M., Hennecke, H., and Fischer, H. M. (2006) The iron control element, acting in positive and negative control of iron-regulated *Bradyrhizobium*

Downloaded from http://www.jbc.org/ at HOKKAIDO DAIGAKU on October 11, 2020

japonicum genes, is a target for the Irr protein. *J. Bacteriol.* **188,** 733–744 CrossRef Medline
5. Yang, J., Sangwan, I., Lindemann, A., Hauser, F., Hennecke, H., Fischer, H. M., and O'Brian, M. R. (2006) Bradyrhizobium japonicum senses iron through the status of haem to regulate iron homeostasis and metabolism. *Mol. Microbiol.* **60,** 427–437 CrossRef Medline
6. Ishikawa, H., Nakagaki, M., Bamba, A., Uchida, T., Hori, H., O'Brian, M. R., Iwai, K., and Ishimori, K. (2011) Unusual heme binding in the bacterial iron response regulator protein: spectral characterization of heme binding to the heme regulatory motif. *Biochemistry* **50,** 1016–1022 CrossRef Medline
7. Kobayashi, K., Nakagaki, M., Ishikawa, H., Iwai, K., O'Brian, M. R., and Ishimori, K. (2016) Redox-dependent dynamics in heme-bound bacterial Iron response regulator (Irr) protein. *Biochemistry* **55,** 4047–4054 CrossRef Medline
8. Qi, Z., Hamza, I., and O'Brian, M. R. (1999) Heme is an effector molecule for iron-dependent degradation of the bacterial iron response regulator (Irr) protein. *Proc. Nat. Acad. Sci. U S A* **96,** 13056–13061 CrossRef Medline
9. Yang, J., Ishimori, K., and O'Brian, M. R. (2005) Two heme binding sites are involved in the regulated degradation of the bacterial iron response regulator (Irr) protein. *J. Biol. Chem.* **280,** 7671–7676 CrossRef Medline
10. Botello-Morte, L., Pellicer, S., Sein-Echaluce, V. C., Contreras, L. M., Neira, J. L., Abian, O., Velazquez-Campoy, A., Peleato, M. L., Fillat, M. F., and Bes, M. T. (2016) Cysteine mutational studies provide insight into a thiol-based redox switch mechanism of metal and DNA binding in FurA from *Anabaena* sp. PCC 7120. *Antioxid. Redox. Signal.* **24,** 173–185 CrossRef Medline
11. Rodionov, D. A., Gelfand, M. S., Todd, J. D., Curson, A. R., and Johnston, A. W. (2006) Computational reconstruction of iron- and manganese-responsive transcriptional networks in alpha-proteobacteria. *PLoS Comput. Biol.* **2,** e163 CrossRef Medline
12. Sangwan, I., Small, S. K., and O'Brian, M. R. (2008) The *Bradyrhizobium japonicum* Irr protein is a transcriptional repressor with high-affinity DNA-binding activity. *J. Bacteriol.* **190,** 5172–5177 CrossRef Medline
13. Chen, J.-J., and Londo, I. M. (1995) Regulation of protein synthesis by heme-regulated eIF-2a kinase. *Trends Biochem. Sci.* **20,** 105–108 CrossRef
14. Zhang, L., and Guarente, L. (1995) Heme binds to a short sequence that serves a regulatory function in diverse proteins. *EMBO J.* **14,** 313–320 CrossRef Medline
15. Yang, J., Kim, K. D., Lucas, A., Drahos, K. E., Santos, C. S., Mury, S. P., Capelluto, D. G., and Finkielstein, C. V. (2008) A novel heme-regulatory motif mediates heme-dependent degradation of the circadian factor period 2. *Mol. Cell. Biol.* **28,** 4697–4711 CrossRef Medline
16. Puri, S., Hohle, T. H., and O'Brian, M. R. (2010) Control of bacterial iron homeostasis by manganese. *Proc. Natl. Acad. Sci. U S A* **107,** 10691–10695 CrossRef Medline
17. Deng, Z., Wang, Q., Liu, Z., Zhang, M., Machado, A. C., Chiu, T. P., Feng, C., Zhang, Q., Yu, L., Qi, L., Zheng, J., Wang, X., Huo, X., Qi, X., Li, X., *et al.* (2015) Mechanistic insights into metal ion activation and operator recognition by the ferric uptake regulator. *Nat. Commun.* **6,** 7642 CrossRef Medline
18. Perard, J., Coves, J., Castellan, M., Solard, C., Savard, M., Miras, R., Galop, S., Signor, L., Crouzy, S., Michaud-Soret, I., and de Rosny, E. (2016) Quaternary structure of Fur proteins, a new subfamily of tetrameric proteins. *Biochemistry* **55,** 1503–1515 CrossRef Medline
19. Golynskiy, M. V., Gunderson, W. A., Hendrich, M. P., and Cohen, S. M. (2006) Metal binding studies and EPR spectroscopy of the manganese transport regulator MntR. *Biochemistry* **45,** 15359–15372 CrossRef Medline
20. Mills, S. A., and Marletta, M. A. (2005) Metal binding characteristics and role of iron oxidation in the ferric uptake regulator from Escherichia coli. *Biochemistry* **44,** 13553–13559 CrossRef Medline
21. Qi, Z., and O'Brian, M. R. (2002) Interaction between the bacterial iron response regulator and ferrochelatase mediates genetic control of heme biosynthesis. *Mol. Cell* **9,** 155–162 CrossRef Medline
22. D'Autréaux, B., Pecqueur, L., Gonzalez de Peredo, A., Diederix, R. E. M., Caux-Thang, C., Tabet, L., Bersch, B., Forest, E., and Michaud-Soret, I. (2007) Reversible redox- and zinc-dependent dimerization of the *Escherichia coli* Fur protein. *Biochemistry* **46,** 1329–1342 CrossRef Medline
23. Pecqueur, L., D'Autreaux, B., Dupuy, J., Nicolet, Y., Jacquamet, L., Brutscher, B., Michaud-Soret, I., and Bersch, B. (2006) Structural changes of *Escherichia coli* ferric uptake regulator during metal-dependent dimerization and activation explored by NMR and X-ray crystallography. *J. Biol. Chem.* **281,** 21286–21295 CrossRef Medline
24. Dian, C., Vitale, S., Leonard, G. A., Bahlawane, C., Fauquant, C., Leduc, D., Muller, C., de Reuse, H., Michaud-Soret, I., and Terradot, L. (2011) The structure of the *Helicobacter pylori* ferric uptake regulator Fur reveals three functional metal binding sites. *Mol. Microbiol.* **79,** 1260–1275 CrossRef Medline
25. Pohl, E., Haller, J. C., Mijovilovich, A., Meyer-Klaucke, W., Garman, E., and Vasil, M. L. (2003) Architecture of a protein central to iron homeostasis: crystal structure and spectroscopic analysis of the ferric uptake regulator. *Mol. Microbiol.* **47,** 903–915 CrossRef Medline
26. Bsat, N., and Helmann, J. D. (1999) Interaction of *Bacillus subtilis* Fur (ferric uptake repressor) with the *dhb* operator in vitro and in vivo. *J. Bacteriol.* **181,** 4299–4307 CrossRef Medline
27. Outten, C. E., and O'Halloran T. V. (2001) Femtomolar sensitivity of metalloregulatory proteins controlling zinc homeostasis. *Science* **292,** 2488–2492 CrossRef Medline
28. Lee, J.-W., and Helmann, J. D. (2007) Functional specialization within the Fur family of metalloregulators. *Biometals* **20,** 485–499 CrossRef Medline
29. Jacquamet, L., Traoré, D. A. K., Ferrer, J. L., Proux, O., Testemale, D., Hazemann, J. L., Nazarenko, E., El Ghazouani, A., Caux-Thang, C., Duarte, V., and Latour, J. M. (2009) Structural characterization of the active form of PerR: insights into the metal-induced activation of PerR and Fur proteins for DNA binding. *Mol. Microbiol.* **73,** 20–31 CrossRef Medline
30. Ahmad, R., Brandsdal, B. O., Michaud-Soret, I., and Willassen, N. P. (2009) Ferric uptake regulator protein: binding free energy calculations and per-residue free energy decomposition. *Proteins* **75,** 373–386 CrossRef Medline
31. Kitatsuji, C., Izumi, K., Nambu, S., Kurogochi, M., Uchida, T., Nishimura, S-I., Iwai, K., O'Brian, M. R., Ikeda-Saito, M., and Ishimori, K. (2016) Protein oxidation mediated by heme-induced active site conversion specific for heme-regulated transcription factor, iron response regulator. *Sci. Rep.* **6,** 18703 CrossRef Medline
32. Iwai, K., Drake, S. K., Wehr, N. B., Weissman, A. M., LaVaute, T., Minato, K., Klausner, R. D., Levine, R. L., and Rouault, T. A. (1998) Iron-dependent oxidation, ubiquitination, and degradation of iron regulatory protein 2: implications for degradation of oxidized proteins. *Proc. Natl. Acad. Sci. U S A* **95,** 4924– 4928 CrossRef Medline
33. Yamanaka, K., Ishikawa, H., Megumi, Y., Tokunaga, F., Kanie, M., Rouault, T. A., Morishima, I., Minato, N., Ishimori, K., and Iwai, K. (2003) Identification of the ubiquitin-protein ligase that recognizes oxidized IRP2. *Nat. Cell Biol.* **5,** 336–340 CrossRef Medline
34. Nishitani, Y., Okutani, H., Takeda, Y., Uchida, T., Iwai, K., and Ishimori, K. (2019) Specific heme binding to heme regulatory motifs in iron regulatory proteins and its functional significance. *J. Inorg. Biochem.* **198,** 110726 CrossRef Medline
35. Halliwell, B., and Aruoma, O. I. (1991) DNA damage by oxygen-derived species: its mechanism and measurement in mammalian systems. *FEBS Lett.* **281,** 9–19 CrossRef Medline
36. Saito, T., Wormald, M. R., and Williams, R. J. P. (1991) Some structural features of the iron-uptake regulation protein. *Eur. J. Biochem.* **197,** 29–38 CrossRef Medline
37. Jaggavarapu, S., and O'Brian, M. R. (2014) Differential control of *Bradyrhizobium japonicum* iron stimulon genes through variable affinity of the iron response regulator (Irr) for target gene promoters and selective loss of activator function. *Mol. Microbiol.* **92,** 609–624 CrossRef Medline
38. Gill, S. C., and Hippel, P. H. V. (1989) Calculation of protein extinction coefficients from amino acid sequence data. *Anal. Biochem.* **182,** 319–326 CrossRef Medline
39. Schlüter, H., and Zidek, W. (1993) Application of non-size-related separation effects to the purification of biologically active substances with a size-exclusion gel. *J. Chromatogr.* **639,** 17–22 CrossRef

Downloaded from http://www.jbc.org/ at HOKKAIDO DAIGAKU on October 11, 2020

Mechanistic insights into heme-mediated transcriptional regulation via a bacterial manganese-binding iron regulator, iron response regulator (Irr)

Dayeon Nam, Yuki Matsumoto, Takeshi Uchida, Mark R. O'Brian and Koichiro Ishimori

J. Biol. Chem. 2020, 295:11316-11325.
doi: 10.1074/jbc.RA119.011855 originally published online June 17, 2020

Access the most updated version of this article at doi: 10.1074/jbc.RA119.011855

Alerts:
- When this article is cited
- When a correction for this article is posted

Click here to choose from all of JBC's e-mail alerts

This article cites 39 references, 11 of which can be accessed free at
http://www.jbc.org/content/295/32/11316.full.html#ref-list-1

Downloaded from http://www.jbc.org/ at HOKKAIDO DAIGAKU on October 11, 2020